

This is the final peer-reviewed accepted manuscript of:

Cingolani A.; Zanutti V.; Zacchini S.; Massi M.; Simpson P. V.; Maheshkumar Desai N.; Casari I.; Falasca M.; Rigamonti L.; Mazzoni R. "Synthesis, reactivity and preliminary biological activity of iron(0) complexes with cyclopentadienone and amino-appended N-heterocyclic carbene ligands", Appl Organometal Chem. 2019;33:e4779.

The final published version is available online at: <https://doi.org/10.1002/aoc.4779>

Rights / License: Licenza per Accesso Aperto. Creative Commons Attribuzione - Non commerciale - Non opere derivate 4.0 (CCBYNCND)

The terms and conditions for the reuse of this version of the manuscript are specified in the publishing policy. For all terms of use and more information see the publisher's website.

This item was downloaded from IRIS Università di Bologna (<https://cris.unibo.it/>)

When citing, please refer to the published version.

Synthesis, reactivity and preliminary biological activity of iron(0) complexes with cyclopentadienone and amino-appended *N*-heterocyclic carbene ligands

Andrea Cingolani,¹ Valerio Zanotti,¹ Stefano Zacchini,¹ Massimiliano Massi,² Peter V. Simpson,² Nima M. Desai,³ Ilaria Casari,³ Marco Falasca,³ Luca Rigamonti,^{4,*} and Rita Mazzoni^{1,*}

¹ Dipartimento di Chimica Industriale “Toso Montanari”, Università degli Studi di Bologna, viale Risorgimento 4, 40136 Bologna, Italy.

² School of Molecular and Life Science - Curtin Institute for Functional Molecules and Interfaces, Curtin University, GPO Box U1987, Perth 6845, Western Australia, Australia.

³ Curtin Health Innovation Research Institute, Curtin University, Perth 6102, Western Australia, Australia.

⁴ Dipartimento di Scienze Chimiche e Geologiche, Università degli Studi di Modena e Reggio Emilia, via G. Campi 103, 41125 Modena, Italy.

Correspondence

Rita Mazzoni, Dipartimento di Chimica Industriale “Toso Montanari”, Università degli Studi di Bologna, viale Risorgimento 4, 40136 Bologna, Italy.

E-mail: rita.mazzoni@unibo.it

ABSTRACT

Neutral and cationic cyclopentadienone (CpO) *N*-heterocyclic carbene (NHC) *bis*-carbonyl iron(0) complexes bearing, appended to the NHC ligand, either a terminal amino group on the lateral chain, $[\text{Fe}(\eta^4\text{-CpO})(\text{CO})_2(\kappa\text{C-NHC}(\text{CH}_2)_n\text{NH}_2)]$ with $n = 2$ (**2a**) and 3 (**2b**), or a cationic NMe_3^+ fragment, $[\text{Fe}(\eta^4\text{-CpO})(\text{CO})_2(\kappa\text{C-NHC}(\text{CH}_2)_2\text{NMe}_3)](\text{I})$ (**3**), were prepared and characterized in terms of their structure, stability and reactivity. The photochemical properties of **2a** and **2b** were examined both in organic solvents and in water, revealing the photoactivated release of one CO ligand followed by the formation of the chelated complex $[\text{Fe}(\eta^4\text{-CpO})(\text{CO})(\kappa^2\text{C,N-NHC}(\text{CH}_2)_2\text{NH}_2)]$ (**4**), whose molecular structure was confirmed by single crystal X-ray diffraction studies. This metallacyclization occurs only in the case of **2a**, with the ethylene spacer between NHC ring and NH_2 group in the lateral chain, allowing the formation of a stable 6-membered ring. On the other hand, **2b** undergoes decomposition upon irradiation. The reactivity in aqueous solutions revealed the chemical speciation of the complexes at different pH and especially under physiological conditions (phosphate buffer solution at pH 7.4 and 37 °C). The lack of data on the biological properties of iron(0) complexes prompted us to preliminarily investigate their cytotoxicity against model cancer cells (AsPC-1 and HPAF-II), along with a determination of their lipophilicity.

KEYWORDS

Iron(0) complexes, cyclopentadienone, *N*-heterocyclic carbene, photoactivation, cytotoxicity

1 INTRODUCTION

Since the discovery that metals play a crucial role in several bio-relevant reactions, coordination compounds, including organometallic complexes, have been used in medicine as both diagnostic and therapeutic agents.^[1-3] One area that has certainly received a significant attention is the application of coordination and organometallic complexes as drugs or prodrugs in the cancer treatment.^[4-11] The readily available and inexpensive iron is a good candidate as a key component in many important biological processes,^[12] and ferrocene derivatives are among the most studied iron complexes for their bio-inorganic properties related to their reactivity and electrochemical properties.^[13-19] Mechanistic studies of ferrocifens highlighted cytostatic properties on tumors, thus causing death of cells by senescence. The presence of side-chain amine groups on ferrocifen complexes leads to major toxicity,^[19] similar to the one observed with other metallocenes.^[20] Extending the promising results using metallocenes, half sandwich iron(II) cyclopentadienyl complexes (e.g. $[\text{Fe}(\eta^5\text{-C}_5\text{H}_5)\text{L}(\text{P-P})]$ with L = imidazole, P-P = chelating diphosphine) have also been recently studied as anticancer drugs, exhibiting cytotoxicity against several human carcinoma cell lines such as the ovarian A2780, breast MCF7, cervical HeLa and colorectal cells.^[21-23] To the best of our knowledge, only one iron(0) complex showing cytotoxic activity on cultivated BJAB mock cells has been reported. In this example, a tris-carbonyliron(0) moiety is coordinated to variously functionalized nucleosides in order to obtain cytostatic and apoptosis-inducing agents, where the metal-carbonyl fragment plays an essential role for the biological function.^[24]

The current state-of-the-art reveals that the design of iron complexes containing ligands able to tune both their solubility in water and electronic properties is still a challenge for the development of bio-active organometallic compounds. Within this field, our group recently developed a straightforward pathway toward the synthesis of a new family of iron(0) complexes where the combination of

cyclopentadienone (CpO), *N*-heterocyclic carbene (NHC) and carbonyl ligands were exploited.^[25] The CpO moiety induces efficient tuning of electronic properties of the metal centers acting as a non-innocent ligand in redox bifunctional catalysis.^[26,27] On the other hand, NHCs can nowadays be considered ubiquitous as ancillary ligands, since they are easy to prepare and can be variously functionalized in order to change steric, electronic and solubility properties of complexes. Indeed, transition metal NHC complexes have found wide application in both catalysis and bioinorganic chemistry.^[28–32] In particular, several examples of these complexes have been found active as cytotoxic agents.^[33–41]

Herein we describe the functionalization of CpO-NHC-*bis*-carbonyl iron(0) complexes, by addition of lateral chains with a terminal amino group to the NHC ligand and yielding compounds of general formula $[\text{Fe}(\eta^4\text{-CpO})(\text{CO})_2(\kappa\text{C-NHC}(\text{CH}_2)_n\text{NH}_2)]$ with $n = 2$ (**2a**), 3 (**2b**), and $[\text{Fe}(\eta^4\text{-CpO})(\text{CO})_2(\kappa\text{C-NHC}(\text{CH}_2)_2\text{NMe}_3)](\text{I})$ (**3**), which show increasing solubility in water. This combination of ligands is useful in order to stabilize the iron(0) oxidation state,^[25,42] and such type of complexes have never been assessed for potential biological applications. Nevertheless, these compounds bring both the metal-carbonyl fragment and the terminal lateral amino chain, which have shown to be able to enhance cytotoxicity.^[19,24] Compound **2a** display the photodissociation of a CO ligand, yielding $[\text{Fe}(\eta^4\text{-CpO})(\text{CO})(\kappa^2\text{C,N-NHC}(\text{CH}_2)_2\text{NH}_2)]$ (**4**), whose molecular structure has been confirmed by X-ray crystallography. The kinetic stability of the new amino-appended complexes in saline phosphate buffer solution (saline PBS) at pH = 7.4, their acid-base properties and lipophilicity character will be presented and discussed. Finally, preliminary *in vitro* tests against AsPC-1 and HPAF-II pancreatic cancer cells as well as healthy human embryonic kidney HEK-293 are reported.

2 EXPERIMENTAL SECTION

2.1 Materials and methods

All reactions were carried out under a nitrogen atmosphere, using standard Schlenk techniques. Glassware was oven dried before use. Dichloromethane (CH₂Cl₂), tetrahydrofuran (THF), diethyl ether (Et₂O), petroleum ether, referring to a fraction of bp 60-80 °C, toluene and acetonitrile (CH₃CN) were dried and distilled prior to use. *n*-hexane was degassed and stored under inert atmosphere on molecular sieves. Other solvents such as ethylacetate (EtOAc), ethanol (EtOH), methanol (MeOH), CDCl₃ (Sigma Aldrich) were employed without further purification. Reagents HBF₄ (ether complex), Na₂CO₃, K₂CO₃, KOH, Na₂SO₄, MeI, trimethylamine-N-oxide and Ag₂O were used as received by Sigma Aldrich or Alfa Aesar. Compounds triscarbonyl-(η⁴-3,4-bis(4-methoxyphenyl)-2,5-diphenylcyclopenta-2,4-dienone)iron,^{[25],[43-45]} 1-(3-BOC-aminopropyl)-imidazole^[46] and dicarbonyl-(2,4-bis(trimethylsilyl)bicyclo[3.3.0]nona-1,4-dien-3-one)[1-(2-BOC-aminoethyl)-3-methylidene]iron (**1a**)^[25] were synthesized as reported in the literature. The NMR spectra were recorded using Varian Inova 300 (¹H, 300.1; ¹³C, 75.5 MHz), Varian Mercury Plus VX 400 (¹H, 399.9; ¹³C, 100.6 MHz), Varian Inova 600 (¹H, 599.7; ¹³C, 150.8 MHz) spectrometers at 298 K; chemical shifts were referenced internally to residual solvent peaks. Infrared spectra were recorded at 298 K on a Perkin-Elmer Spectrum Two spectrophotometer. ESI-MS spectra were recorded on a Waters Micromass ZQ 4000 with samples dissolved in MeOH. Elemental analyses were performed on a Thermo-Quest Flash 1112 Series EA instrument. UV irradiation was performed by using a commercial Hg lamp (365 nm, 125 W). UV-visible spectra were recorded on an Agilent Cary 100 UV-vis spectrophotometer.

2.2 Synthesis of 1-(3-BOC-aminopropyl)-3-methylimidazolium iodide

An excess of CH₃I (0,84 mL, 13,5 mmol) was added to a solution of 1-(3-BOC-aminopropyl)-imidazole (1g, 2,7 mmol) in CH₂Cl₂ (10 mL) and stirred overnight. Solvent was removed under reduced pressure and the residue was extensively washed with Et₂O, obtaining the title compound as yellow oil in quantitative yield. ¹H NMR (300.1 MHz, 298 K, CDCl₃): δ (ppm) 9.75 (s, 1H, NCHN), 7.69 (s, 1H, CH_{im}), 7.49 (s, 1H, CH_{im}), 5.47 (s, 1H, NH), 4.36 (t, 2H, *J*_{H,H} = 6.31 Hz, NCH₂), 4.04 (s, 3H, NCH₃), 3.14 (q, 2H, *J*_{H,H} = 5.92 Hz, CH₂NHBOC), 2.12 (quint, 2H, *J*_{H,H} = 6.67 Hz, CH₂), 1.37 (s, 1H, CH₃Boc). ¹³C NMR (75.5 MHz, 298 K, CDCl₃): δ (ppm) 156.5 (C=O_{Boc}), 136.8 (NCHN), 123.4 (CH_{im}), 122.8 (CH_{im}), 79.3 (C_q, Boc), 47.3 (NCH₂), 36.9 (CH₂NHBOC), 36.6 (NCH₃), 30.6 (CH₂), 28.26 (CH₃, Boc). ESI-MS (MeOH): *m/z* 240 [M]⁺. Anal. Calcd (%) for C₁₂H₂₂N₃O₂: C, 59.97; H, 9.23; N, 17.48. Found: C, 60.07; H, 9.31; N 17.11.

2.3 Synthesis of dicarbonyl-(2,4-bis(trimethylsilyl)bicyclo[3.3.0]nona-1,4-dien-3-one)[1-(3-BOC-aminopropyl)-3-methylidene]iron (1b)

In a dried 100 mL Schlenk flask, 1-(3-BOC-aminopropyl)-3-methylimidazolium iodide (0.145 g, 0.395 mmol) and silver oxide (0.110 g, 0.474 mmol), triscarbonyl-(η⁴-3,4-bis(4-methoxyphenyl)-2,5-diphenylcyclopenta-2,4-dienone)iron (0.150 g, 0.359 mmol) and trimethylamine-N-oxide (0.041 g, 0.593 mmol) were dissolved in CH₃CN (20 mL). The reaction mixture was stirred at room temperature and protected from light for 1 h, and then solvent was removed under reduced pressure. The solid was redissolved in toluene (40 mL) and left under reflux for 1 h. At the end of reaction time, solvent was removed under reduced pressure and the crude product was purified by column chromatography on neutral alumina using CH₂Cl₂/EtOAc (1:1) affording the titled complex as yellow powder (42%). ¹H NMR (399.9 MHz, 298 K, CDCl₃): δ (ppm) 7.12 (s, 1H, CH_{NHC}), 7.01 (s, 1H, CH_{NHC}), 4.26 (t, 2H, *J*_{H,H} = 7.1 Hz, NCH₂), 3.92 (s, 3H, NCH₃), 3.28 (br, 2H, CH₂), 3.09 (br, 2H, CH₂), 2.43-2.40 (m, 4H, CH₂),

2.01 (m, 2H, CH₂), 1.83-1.77 (m, 4H, CH₂), 0.15 (s, 18H, CH₃TMS). ¹³C NMR (150.8 MHz, 298 K, CDCl₃): δ (ppm) 217.1 (CO), 184.1 (C_{carb}), 168.9 (C=O_{Cp}), 156.1 (C=O_{BOC}), 124.4 (CH_{NHC}), 122.1 (CH_{NHC}), 104.1 (C_{3,4}, Cp), 79.3 (C_q, BOC), 71.6 (C_{2,5}, Cp), 49.3 (-NCH₂-), 40.1 (-NCH₃), 39.5 (-NCH₂-), 28.4 (CH₃, BOC), 24.5 (-CH₂), 22.5 (-CH₂), 0.20 (CH₃, TMS). IR (CH₂Cl₂, cm⁻¹): ν 1986, 1930. ESI-MS (MeOH): *m/z* 630 [M + H]⁺, 652 [M + Na]⁺. Anal. Calcd (%) for C₂₉H₄₇FeN₃O₅Si₂ (629.73): C, 55.31; H, 7.52; N, 6.67. Found: C, 55.99; H, 7.51; N 6.66.

2.4 Synthesis of dicarbonyl-(2,4-bis(trimethylsilyl)bicyclo[3.3.0]nona-1,4-dien-3-one)[1-(2-aminoethyl)-3-methylidene]iron (2a)

In a dried 25 mL Schlenk flask, **1a** (0.058 g, 0.094 mmol) was dissolved in Et₂O (2 mL) and HBF₄ (0.071 mL, 0.515 mmol) was added dropwise. The reaction mixture was stirred at room temperature for 1 h. The precipitate was dissolved in CH₂Cl₂ and the excess of HBF₄ was neutralized with a saturated solution of sodium carbonate till pH = 7-8. The aqueous phase was extracted with CH₂Cl₂, the organic phase was washed with a potassium hydroxide solution (1.5 M, 3 × 10 mL). The organic phase was dried with sodium sulfate and filtrated. Solvent was removed under reduced pressure yielding a yellow solid (73.4%). ¹H NMR (399.9 MHz, 298 K, CDCl₃): δ (ppm) 7.20 (s, 1H, -CH_{NHC}), 7.02 (s, 1H, -CH_{NHC}), 4.31 (t, 2H, *J*_{H,H} = 6.6 Hz, CH₂), 3.92 (s, 6H, -NCH₃), 3.13 (t, 2H, *J*_{H,H} = 5.7 Hz, -CH₂), 2.43 (m, 4H, CH₂), 1.92-1.77 (m, 4H, CH₂), 0.16 (s, 18H, CH₃TMS). ¹³C NMR (150.8 MHz, 298 K, CDCl₃): δ (ppm) 217.4 (CO), 184.9 (C_{carb}), 176.3 (C₁=O, Cp), 124.1 (CH_{NHC}), 122.1 (CH_{NHC}), 103.9 (C_{3,4}, Cp), 71.5 (C_{2,5}, Cp), 53.9 (-NCH₂-), 42.5 (-NCH₂-), 40.2 (-NCH₃), 24.6 (-CH₂), 22.5 (-CH₂), 0.24 (CH₃TMS). IR (CH₂Cl₂, cm⁻¹) ν (CO) 1982, 1922. ESI-MS (MeOH): *m/z* 459 [M + H - 2CO]⁺, 488 [M + H - CO]⁺, 516 [M + H]⁺, 538 [M + Na]⁺. Anal. Calcd (%) for C₂₃H₃₇FeN₃O₃Si₂ (515.58): C, 53.58; H, 7.23; N, 8.15. Found: C, 53.69; H, 7.24; N 8.14.

2.5 Synthesis of dicarbonyl-(2,4-bis(trimethylsilyl)bicyclo[3.3.0]nona-1,4-dien-3-one)[1-(3-aminopropyl)-3-methylidene]iron (2b)

In a dried 25 mL Schlenk flask, **1b** (0.094 g, 0.150 mmol) was dissolved in Et₂O (2 mL) and HBF₄ (0.103 mL, 0.750 mmol) was added dropwise. The reaction mixture was stirred at room temperature for 1 h. The precipitate was dissolved in CH₂Cl₂ and the excess of HBF₄ was neutralized with a saturated solution of sodium carbonate till pH = 7-8. The aqueous phase was extracted with CH₂Cl₂, the organic phase washed with a potassium hydroxide solution (1.5 M, 3 × 10 mL). Organic phase was dried with sodium sulfate and filtrated. Solvent was removed under reduced pressure to leave a yellow solid (75%). ¹H NMR (399.9 MHz, 298 K, CD₃Cl): δ (ppm) 7.06 (s, 1H, -CH_{NHC}), 7.01 (s, 1H, -CH_{NHC}) 4.30 (t, 2H, , *J*_{H,H} = 7.5 Hz, CH₂), 3.94 (s, 3H, -NCH₃), 2.88 (t, 2H, *J*_{H,H} = 5.9 Hz, -CH₂), 2.41 (m, 4H, CH₂), 1.95 (quint, 2H, *J*_{H,H} = 6.4 Hz, CH₂), 1.85-1.77 (m, 4H, CH₂), 0.16 (s, 18H, CH₃TMS). ¹³C NMR (150.8 MHz, 298 K, CDCl₃): δ (ppm) 217.2 (CO), 184.5 (C_{carb}), 176.8 (C_{1=O}, Cp), 124.2 (CH_{NHC}), 121.9 (CH_{NHC}), 104.0 (C_{3,4}, Cp), 70.9 (C_{2,5}, Cp), 49.6 (-NCH₂-), 40.2 (-NCH₂-), 39.3 (-NCH₃), 31.6 (CH₂), 24.5 (-CH₂), 22.6 (-CH₂), 0.21 (CH₃TMS). IR (CH₂Cl₂, cm⁻¹) ν 1986, 1930. ESI-MS (MeOH): *m/z* 530 [M + H]⁺, 552 [M + Na]⁺. Anal. Calcd (%) for C₂₄H₃₉FeN₃O₃Si₂ (524.61): C, 54.43; H, 7.42; N, 7.93. Found: C, 54.22; H, 7.43; N 7.94.

2.6 Synthesis of dicarbonyl-(2,4-bis(trimethylsilyl)bicyclo[3.3.0]nona-1,4-dien-3-one)[1-(2-*N,N,N*-trimethylaminoethyl)-3-methylidene]iron iodide (3)

In a dried 25 mL Schlenk flask, **2a** (0.097 g, 0.187 mmol) and potassium carbonate (0.116 g, 0.842 mmol) were dissolved in CH₂Cl₂ (2 mL) and CH₃I (0.105 mL, 1.683 mmol) was added dropwise. The reaction mixture was stirred at room temperature for 1 day. The solution was filtered and the solvent was removed under reduced pressure. The crude product was purified by column chromatography on neutral alumina using CH₂Cl₂/MeOH (40:5) affording the title compound in quantitative yield as a yellow solid. ¹H NMR

(399.9 MHz, 298 K, DMSO): δ (ppm) 7.63 (s, 1H, -CH_{NHC}), 7.60 (s, 1H, -CH_{NHC}), 4.67 (t, 2H $J_{H,H} = 8.1$ Hz, CH₂), 3.88 (s, 3H, -NCH₃), 3.69 (t, 2H, $J_{H,H} = 7.7$ Hz, -CH₂), 3.22 (s, 9H, CH₃), 2.41-2.20 (m, 4H, CH₂), 1.81-1.74 (m, 4H, CH₂), 0.08 (s, 18H, CH₃TMS). ¹³C NMR (150.8 MHz, 298 K, DMSO): δ (ppm) 217.7 (CO), 182.8 (C_{carb}), 177.6 (C_{1=O}, Cp), 126.0 (CH_{im}), 123.6 (CH_{im}), 105.3 (C_{3,4}, Cp), 68.3 (C_{2,5}, Cp), 63.5 (-NCH₂), 53.2 (-N⁺CH₃), 44.1 (-NCH₂), (-NCH₃, not visible), 23.8 (-CH₂), 22.0 (-CH₂), 0.03 (CH₃TMS). IR (CH₂Cl₂, cm⁻¹) ν (CO) 1978, 1917. ESI-MS (MeOH): m/z 558 [M]⁺. Anal. Calcd (%) for C₂₆H₄₄FeN₃O₃Si₂ (558.67): C, 45.55; H, 6.47; N, 6.13. Found: C, 45.73; H, 6.49; N 6.14.

2.7 Synthesis of carbonyl-(2,4-bis(trimethylsilyl)bicyclo[3.3.0]nona-1,4-dien-3-one)[1-(2-aminoethyl)-3-methylidene]iron (4)

In a dried 50 mL Schlenk flask, **2a** (0.040 g, 0.096 mmol) was dissolved in toluene (40 mL). The reaction solution was irradiated under UV radiation (325 nm) at room temperature for 90 minutes and then solvent was removed under reduced pressure. The residue was dissolved in CH₃CN and the product purified by precipitation with *n*-hexane, to leave a red solid identified as **4** (65%). ¹H NMR (399.1 MHz, 298 K, CDCl₃): δ (ppm) 6.91 (m, 2H, CH_{NHC}), 3.91-3.81 (m, 2H, CH₂), 3.83 (s, 3H, CH₃), 3.28 (m, 1H, CH₂), 3.01(m, 1H, CH₂), 2.47-2.16 (m, 4H, CH₂), 1.65-1.56 (m, 4H, CH₂), 0.17 (s, 9H, CH₃TMS), -0.02 (s, 9H, CH₃TMS). ¹³C NMR (150.8 MHz, 298 K, CDCl₃): δ (ppm) 220.0 (CO), 192.7 (C_{carb}), 168.3 (C=O_{Cp}), 122.8 (CH_{NHC}), 122.2 (CH_{NHC}), 101.2 (C_q), 93.8 (C_q) 73.4 (C_q), 59.4 (C_q) 49.7 (CH₂), 41.9 (CH₂), 37.6 (CH₃), 25.3 (CH₂), 23.7 (CH₂), 22.6 (CH₂), 22.1 (CH₂), 0.90 (CH₃TMS), 0.64 (CH₃TMS). IR (CH₂Cl₂, cm⁻¹): ν 1879. ESI-MS (MeOH): m/z 488 [M + H]⁺, 510 [M + Na]⁺. Anal. Calcd (%) for C₂₂H₃₇FeN₃O₂Si₂ (487.57): C, 54.19; H, 7.65; N, 8.62. Found: C, 54.29; H, 7.64; N 8.63.

2.8 X-ray crystallography

Crystal data and collection details for **4** are reported in Table S1 in Supporting Information (SI). The diffraction experiments were carried out on a Bruker APEX II diffractometer equipped with a PHOTON100 detector and using Mo-K α radiation at 298 K. Data were corrected for Lorentz polarization and absorption effects (empirical absorption correction SADABS.^[47] Structure was solved by direct methods and refined by full-matrix least-squares based on all data using F^2 .^[48] H-atoms were placed in calculated positions, and refined isotropically using a riding model, unless otherwise stated. H(3a) and H(3b) bonded to N(3) were preliminarily located in the electron-density map but, then, refined by a riding model. All non-hydrogen atoms were refined with anisotropic displacement parameters. Compound **4** co-crystallizes with one CH₂Cl₂ molecule per formula unit. Even though the CH₂Cl₂ molecule was preliminarily located in the Fourier difference map, it was not possible to refine it. Thus, it was treated using the SQUEEZE routine of PLATON.^[49,50]

2.9 UV-visible spectrophotometric studies

Kinetic stability and CO release in physiological conditions: The stability of **2a**, **2b**, **3** and **4** at 37 °C in darkness was evaluated by UV-vis spectroscopy as a change in absorbance in the 250–550 nm range over a period of 72 h. Solutions in the $1\text{--}5 \times 10^{-5}$ mol L⁻¹ concentration range were prepared in phosphate buffer solution (PBS) 0.01 mol L⁻¹ at pH 7.4 by appropriate dilution of concentrated solutions of the complexes in DMSO (about 10⁻³ mol L⁻¹). A constant ionic strength of 0.1 M was maintained with addition of NaCl in all experiments (saline PBS). UV-visible spectra were also recorded after exposure to the light of the previous diluted solutions of **2a** and **2b** in order to detect the CO release and the closure of the metallacycle in physiological conditions. Stability experiments for **2a** and **4** were also repeated in NaCl 0.1 mol L⁻¹ (saline solution) and distilled water under the sunlight at the same diluted concentrations.

pH-dependent titrations for pK_b determination: Spectrophotometric titrations of **2a**, **2b**, **3** and **4** were performed by dissolving the complexes in DMSO to give a mother solution (about 10^{-3} mol L⁻¹), and then diluting in NaCl 0.1 mol L⁻¹ aqueous solution (final $V = 25$ mL) in order to obtain a final concentration of about 2.5×10^{-5} mol L⁻¹ and to maintain a constant ionic strength in all experiments. The pH value was varied by adding small amounts (10 μ L) of concentrated NaOH or HBF₄ using a micropipette in the 2–13 pH range, thus volume variation was negligible. The UV-visible absorption spectra were recorded for all different pH values and the protonation constants were evaluated as proposed in the literature.^[51]

2.10 Partition coefficients $\log D_{7.4}$ and $\log D_{4.6}$

$\log D_{7.4}$ values, partition coefficient *n*-octanol/water, were determined using the shake-flask method. PBS 10 mM (pH adjusted to 7.4 with HCl) and *n*-octanol were shaken together for 3 days to allow saturation of both phases. Then, 750 μ L of both phases and 50 μ L of a complex stock solution (1 mg in 200 μ L of DMSO) were combined in an Eppendorf tube (2 mL) and shaken in a lab vortex for 10 min (VWR Analogue Vortexer). The emulsion was centrifuged (10 min, 15000 rpm) to separate the two phases. UV-vis absorption data were determined at either 280 or 325 nm for both phases. The aqueous phase was diluted 3-fold while the *n*-octanol phase 20-fold in order to have an absorbance $A < 1$. The $\log D_{7.4}$ values were calculated according to Eq. (1), where f_{dil} is the dilution factor. The given values are the mean of three separate determinations. $\log D_{4.6}$ values were determined following the same procedure of $\log D_{7.4}$, but the water phase was an acetate buffer solution 10 mM (pH adjusted to 4.6 with NaOH).

$$\log D_{7.4-4.6} = \log \left(\frac{A_{octanol} \cdot f_{dil}}{A_{buffer} \cdot f_{dil}} \right) \quad (1)$$

2.11 Cell growth assays and IC₅₀ determination

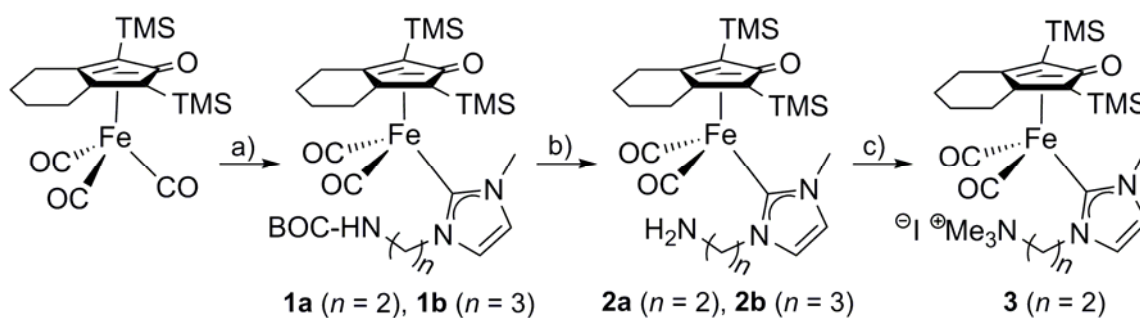
For cell counting, the cell lines were seeded in 12 well plates (50,000 cells per well) and grown in cell culture medium supplemented with 10% Simulated Body Fluid (SBF). After an overnight incubation,

the complete media was replaced with fresh one containing DMSO 0.1%, and the iron complexes at a range of concentrations between 0 and 30 μM . After 72 h of incubation at 37 °C and 5% CO_2 , the cells were washed once in warm PBS, and detached with trypsin-EDTA 0.25% at 37 °C and 5% CO_2 . When a complete cells detachment was achieved, the proteasic activity was stopped with one volume of complete media. The total number of cells per well was quantified by manual cell counting under bright field microscopy using Neubauer or Burker chambers.

3 RESULTS AND DISCUSSION

3.1 Synthesis of the iron complexes and CO release studies

The synthetic approach that allows the addition of a monodentate NHC ligand on *bis*-carbonyl cyclopentadienone iron(0) complexes, developed by our group^[25] is herein exploited in order to prepare a new class of complexes bearing an amine functional group. Specifically, the functionalization of the NHC ligand with an amine-terminated short alkyl chain attached to one of the imidazolium N atoms has led to the isolation of derivatives **2a**, **2b** and **3** (Scheme 1). Complexes **2a** and **2b** were prepared with yields around 70% by deprotection of the corresponding NHBOC-protected complexes **1a**^[25] and **1b** with HBF_4 , followed by neutralization of any unreacted acid. These complexes contain an ethylamino or propylamino lateral chain in **2a** or **2b**, respectively. Complex **2a** was also alkylated using CH_3I to form the cationic **3**, containing a terminal quaternary ammonium group.^[52]

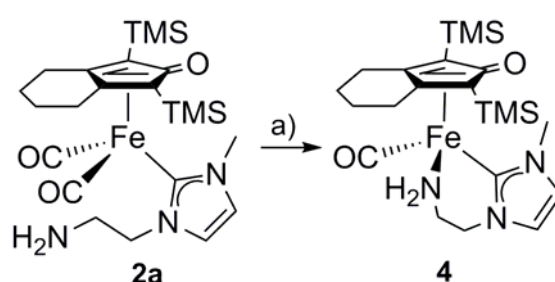


SCHEME 1 Iron(0) complexes with cyclopentadienone and amino-functionalized NHC ligands **1a**, **1b**, **2a**, **2b** and **3** (TMS = trimethylsilyl, BOC = *tert*-butyloxycarbonyl). Reactions conditions: a) 1-(3-BOC-aminoethyl/propyl)-3-methylimidazolium iodide (1.1 eq.), Ag₂O (1.3 eq.), Me₃NO (1.6 eq.), CH₃CN, 1 h, room temperature, toluene, 1 h, reflux; b) i) HBF₄ (5 eq.), Et₂O, 1 h, room temperature, ii) KHCO₃ (pH 7-8); c) CH₃I (9 eq.), K₂CO₃ (6 eq.), CH₂Cl₂, 1 day, room temperature.

All the synthesized compounds were characterized by means of IR, ¹H and ¹³C NMR spectroscopies, ESI-MS spectrometry and elemental analyses (see Experimental Section and Figures S1–S15 in SI). In particular, complexes appear as yellow powders that are stable towards air and moisture while kept in the dark, both in the solid state and in most common organic solvents. ¹³C NMR spectra show the diagnostic signal for the Fe-C_{carbene} at 181-185 ppm, while the CO stretching peaks around 1980 and 1920 cm⁻¹ can be observed in the IR spectra from CH₂Cl₂ solutions.

Compound **2a** shows, upon exposure to sunlight both in solution and in the solid state, a change from yellow to orange. The corresponding changes in the IR spectra suggest the release of a CO ligand. Indeed, upon irradiation (365 nm, 125 W) of a yellow solution of **2a** in toluene, a change to deep red was observed in about 1 hour. The reaction was monitored by IR spectroscopy, where the two carbonyl bands of **2a** ($\nu(\text{CO}) = 1982, 1922 \text{ cm}^{-1}$) slowly disappeared and were replaced by a new single stretching vibration associated with one remaining CO ligand in **4** ($\nu(\text{CO}) = 1879 \text{ cm}^{-1}$) (Scheme 2). ¹³C NMR shows a downfield shift for the C_{carbene} (δ **2a**: 185 ppm vs. **4**: 193 ppm) and an upfield shift for the C=O (δ **2a**:

176 ppm vs. **4**: 168 ppm). Complex **4** could be also isolated as a pure compound by dissolution in CH₃CN and precipitation with *n*-hexane (see Experimental Section and Figures S16–S18 in SI), and it is also air and moisture stable in the solid state and organic solvents (e.g. CH₂Cl₂, toluene, CH₃CN) at room temperature. Interestingly, a toluene solution of **4** under a CO atmosphere (1.5 atm) did not show any reverse reaction to form **2a**, demonstrating the stability of the chelated form.



SCHEME 2 CO release under irradiation and ring closure to form **4**, feasible only for **2a** by the presence of ethylene groups and the formation of a 6-membered metallacycle. Reaction conditions: a) UV radiation (365 nm, 125 W), toluene, 90 minutes, room temperature.

Single crystals of **4** suitable for X-ray diffraction studies were obtained by a double layer of CH₂Cl₂:*n*-hexane. The molecular structure of **4** is reported in Figure 1 and shows the 6-membered metallacycle involving iron and the chelating κ^2 -*C,N*-NHCCH₂CH₂NH₂, as evidenced by the close Fe(1)–N(3) contact [2.0636(16) Å] (see Table S2 in SI for a complete list of bond distances and angles). An intramolecular hydrogen bond is also present between the amino and ketone groups [N(3)–H(3b) 0.89 Å, H(3b)⋯O(2) 2.09 Å, N(3)⋯O(2) 2.845(42) Å, <N(3)H(3b)O(2) 142.2°], which further enhances the stability of the metallacycle. The Fe(1)–C(2) distance [2.2926(17) Å] is significantly longer than Fe(1)–C(3-6) [2.0772(18)–2.1598(19) Å], and C(2)–O(2) [1.271(2) Å] is essentially a double bond.^[53] The Fe(1)–C(17) contact [1.945(2) Å] is in the typical range for the interaction between iron(0) and an *N*-

heterocyclic carbene, ^{[25],[54]} and the overall structure of **4** resembles that of previously reported $[\text{Fe}(\text{CpO})(\text{CO})_2(\text{NHC})]$ analogue of **2a**.^[25]

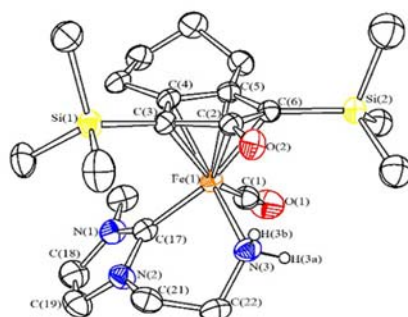


FIGURE 1 Molecular structure of **4** with displacement ellipsoids drawn at the 30% probability level and principal atom labelling; hydrogen atoms are omitted for clarity.

Analogous experiments were performed with **2b**, bearing the propylene amino lateral chain. Leaving the solution of **2b** in toluene under UV irradiation for several hours did not afford the corresponding chelated form, and only the reduction of the CO stretching signals of **2b** could be detected by time. After eight hours of continuous irradiation, **2b** completely decomposed, suggesting that the formation of a metallacycle is favored by the formation of a 6-membered ring, as in the case of **2a** that converts into **4**.

3.2 Kinetic stability and chemical speciation in solution

Complexes **2a** and **2b** are soluble in acidic water (e.g. acetic acid/acetate buffer solution, pH = 4.74, 35.4 mmol/L; 18.5 g/L), but not in neutral or basic medium (pH = 7.4, $< 3.2 \times 10^{-5}$ mmol/L). The cationic NMe_3^+ group in the lateral chain of **3** makes it more soluble in water even at basic pH values (pH = 7.4, 38.2 mmol/L, 26.2 g/L). The stability of **2a**, **2b**, **3** and **4** in aqueous media was investigated by means of UV-visible spectroscopy. The experiments were carried out at 37 °C in darkness in saline PBS.^[55] These conditions were chosen given our interest in investigating the cytotoxicity of these species. The four complexes were mainly found to absorb in the 250–400 nm range, displaying similar spectra with subtle but noticeable differences in the position and intensity of maxima (Figure S19 in SI).

In the case of **2a** and **2b** with the free amino group on the lateral chain and of **3** with the cationic NMe_3^+ fragment we could observe a high stability over a period of 72 h, with a diminishing of only about 10–15% of the intensity in the whole wavelength range, while maintaining the same absorption profile (Figure 2a,b,c). This behavior suggests that the main species in solution remain unaltered. On the other hand, a different behavior is observed for **4** (Figure 2d). In this case, a rapid decrease of the intensity of the band at 270 nm and a slight increase of the band at about 400 nm are observed within few hours of incubation. After 24 hours only further minor differences are detected in the spectra up to a period of 72 hours.

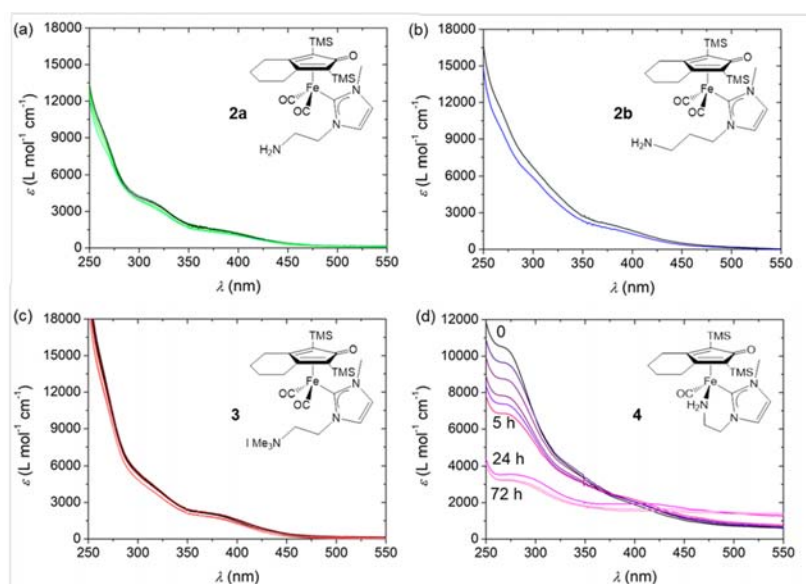


FIGURE 2 Kinetic stability studies through UV-visible spectroscopy of (a) **2a**, (b) **2b**, (c) **3** and (d) **4** at 37 °C in darkness in saline PBS 0.01 mol L⁻¹ at pH 7.4 and constant ionic strength of 0.1 mol L⁻¹ with addition of NaCl, over a period of 72 h: ($t = 0$: black, $t = 72$ h: green, blue, red or violet for **2a**, **2b**, **3** or **4**, respectively).

A UV-vis spectrum very similar to the one generated from **4** in saline PBS in the dark was also obtained by exposing the solution of **2a** in saline PBS to sunlight. The changes in the spectra are again attributed to the first release of a CO ligand from **2a** to generate **4**, which then follows an analogous pathway.

Similar changes did not happen in the case of **2b** under the same conditions, confirming that CO expulsion has to be promoted by the presence of the $(\text{CH}_2)_2\text{NH}_2$ lateral chain also in physiological conditions. Upon repeating stability experiments of **2a** in NaCl 0.1 mol L^{-1} (saline solution) under sunlight for 24 hours, we could again observe a quick change of the absorption spectrum within few hours, and reaching in 24 hours an absorption spectrum very similar to that of **4** in saline PBS (Figure S20 in SI). When the experiments were repeated in distilled water, only a slight diminishing of the intensity of the whole spectrum could be instead observed. All these data suggest that the stable species generated in saline PBS from either **4** in the dark or **2a** under the sunlight might contain a coordinated chloride ion, which is present in more than 1000 molar excess with respect to the iron complexes (this species will be hereafter referred as **4'** for the sake of clarity). This is also confirmed by the fact that **4** in distilled water did not change its absorption spectrum within 24 hours, which suggests that water does not replace the amino ligand in physiological conditions. As a conclusion, chloride ions by themselves are not able to substitute a CO ligand in **2a** even when present in large excess, but only under photoactivation.

Acid-base properties of the compounds were also tested in saline solution by means of UV-visible spectroscopy. Although variations are small, we could observe a dependence of the absorption spectrum of **2b** upon modulation of pH (Figure S21a in SI). By analyzing the changes at different wavelengths (for example 310, 350 and 380 nm, Figure S21b in SI), a sigmoidal titration evolution can be clearly recognized, independently from the selected λ value. From the collected spectra, it is possible to extrapolate a $\text{p}K_{\text{b}}$ value of 9.7(2).^[51] Light sensitivity of **2a**, especially upon pH variation, hampered the collection of reliable data for the $\text{p}K_{\text{b}}$ determination. Nevertheless, thanks to its close chemical resemblance with **2b**, a very similar basicity can be reasonably expected for **2a**. A pH-dependent behavior of the absorption spectra of **4** was also found (Figure S22), for which a very close $\text{p}K_{\text{b}}$ value of 10.0(4)

could be obtained, due to the presence of the free amino group of the open metallacycle in saline solution. The same pH dependence could not be observed in the case of **3** with the cationic NMe_3^+ terminal group. As a consequence, these acid-base equilibria can be assigned to the protonation of the amine group of the lateral chain in **2a** and **2b** and the stabilized species in saline solution **4'** (generated from **4**), which are not protonated at physiological conditions ($\text{pH} = 7.4$) and mostly present as neutral complexes, while **3** is stable in its cationic form.

3.3 Lipophilicity measurements and cytotoxicity

The stability of the complexes in aqueous medium prompted us to investigate their biological behavior in terms of cytotoxicity. Lipophilicity is also an important parameter to evaluate the complexes in a biological context, as it influences the capacity of species to traverse the cellular membrane. The lipophilicity values, measured as their $\log D$ values, were determined by the shake-flask methods (see Experimental Section) and reported in Table 1. For the aqueous phase, a solution at neutral (7.4) or acidic pH (4.6) was employed, and as expected, the lipophilicity values of the complexes change depending on the pH of the solution due to the presence of the amino group. The ammonium salt **3**, which is soluble both in acidic and basic water, shows no difference of $\log D$ values under different pH. Concerning the complex **2b** we can observe that lipophilicity in acidic medium is comparable with the one of **3**, while increasing at physiological pH. These results are both in agreement with the above discussed protonation of amino-group at pH 4.6, and the expected neutral form of **2b** at pH 7.4. **2a** shows a similar behavior as **2b**. Compound **4**, where the amino group chelates the iron center, displays a similar lipophilicity independently to the pH; in fact, for these measurements the water phase was not implemented with NaCl in order to avoid the opening of the metallacycle to generate **4'**.

TABLE 1 LogD values and IC₅₀ (μM) values for **2a**, **2b**, **3** and **4** against pancreatic cancer AsPC-1 and HPAF-II cells, and healthy human embryonic kidney HEK-293 cells (incubation time of 72 h).

Complex	lipophilicity		IC ₅₀		
	logD _{4.6}	logD _{7.4}	AsPC-1	HPAF-II	HEK-293
2a	1.6 ± 0.1	1.97 ± 0.05	4.9 ± 1.5	6.9 ± 0.6	13.3 ± 2.6
2b	1.09 ± 0.07	2.0 ± 0.3	6.6 ± 1.5	6.6 ± 1.5	9.6 ± 2.6
3	0.99 ± 0.05	1.01 ± 0.09	–	–	–
4	2.6 ± 0.2	2.4 ± 0.4	8.8 ± 1.0 ^a	20.7 ± 8.1 ^a	> 30 ^a
Carboplatin	–	–	6.8 ± 2.0 ^b	8.7 ± 4.3 ^b	11.2 ± 3.2 ^c

^a Due to the presence of chloride ions in culture medium, the active species in solution is probably **4'**.

^b Literature data.^[57] ^c Literature data.^[58]

The iron compounds were tested against AsPC-1 pancreatic cancer cells at an initial concentration of 10 μM, to screen for cytotoxic activity. Pancreatic cells were chosen as they are known to be particularly robust.^[46] All the iron compounds, with the exception of **3**, led to a decrease in cell number by 50% or more (relative to controls). Therefore, the IC₅₀ values of these four complexes were measured against AsPC-1 and HPAF-II pancreatic cancer cells, with HEK-293 serving as the healthy cell control (Table 1).

All tested complexes display a cytotoxic activity comparable to carboplatin against AsPC-1 and HPAF-II cells. The complexes show slightly lower activities against healthy HEK-293, although selectivity indices are generally less than 2, suggesting poor selectivity toward cancer cells. An exception is given by **4**, in which the cytotoxicity against ASPC-1 tumor cells is much higher than the one in healthy cells, and this can be tentatively ascribed to the fact that **4** interconverts in the species **4'** in physiological conditions. Given that **2a** and **2b** are neutral at physiological pH as well as in the more acidic pancreatic

cancer cells (pH \approx 6.7)^[56] and **3** is positively charged, it also appears that quaternisation of the pendant amine leads to complete loss of activity. This could be potentially due to the fact that the lower lipophilicity of the cationic species might hinder cellular internalization; however, further studies will help to illustrate this point.

4 CONCLUSIONS

The new organometallic CpO-NHC iron(0) complexes functionalized with a pendant amino group on the NHC ligand here presented have shown that the affinity toward the water phase is highly influenced by the amino group, which is susceptible to protonation below pH 6 (as evidenced by pH titration), or its quaternarization. In fact, alkylation of the amino group to NMe₃⁺ fragment in **3** results in increased water solubility especially at physiological conditions. Noteworthy, **2a**, **2b** and **3** are stable in saline PBS for 72 h in the dark, which ensures their use in cellular tests. On the other hand, leaving the buffer solution of **2a** to sunlight leads to the formation of a novel species. Studying the reactivity of complex **2a** under photolytic conditions also in organic solvents allows to isolate the chelating complex **4**, the stable product of CO release from **2a**, which however appears to be unstable in a saline PBS solution evolving to the same species as **2a**. This thus shows the relevant role of Cl⁻ in the kinetic stability of complexes **2a** and **4**, which actually evolve, in the presence of sunlight, to the same final species **4'**. Finally, the cytotoxicity of the compounds were preliminarily tested against pancreatic cancer AsPC-1 and HPAF-II cells and healthy human embryonic kidney HEK-293 cells, with IC₅₀ values comparable to carboplatin but low selectivity, with the exception of **4**, probably due to its conversion to **4'**. Only ammonium salt **3** was found to be not active. The results of these preliminary studies are promising and warrant further studies, both in assessing the nature of **4'** and in addressing structural modifications in order to enhance the selectivity.

ACKNOWLEDGMENT

The Italian Ministero dell'Istruzione, dell'Università e della Ricerca (MIUR) (PRIN 2015 20154X9ATP_003) and the Università degli Studi di Bologna are acknowledged for financial support.

M.M. wishes to thank the Australian Research Council (ARC) (FT130100033) and Curtin University for funding. Work in the Falasca laboratory was supported by Avner Pancreatic Cancer Foundation.

ORCID

Andrea Cingolani: 0000-0001-7011-7210

Valerio Zanotti: 0000-0003-4190-7218

Stefano Zacchini: 0000-0003-0739-0518

Massimiliano Massi: 0000-0001-6949-4019

Peter V. Simpson: 0000-0002-5701-3203

Marco Falasca: 0000-0002-9801-7235

Luca Rigamonti: 0000-0002-9875-9765

Rita Mazzoni: 0000-0002-8926-9203

REFERENCES

- [1] N. Metzler-Nolte, Z. Guo, *Dalton. Trans.* **2016**, *45*, 12965–12965.
- [2] G. Jaouen, N. Metzler-Nolte, Eds. , *Medicinal Organometallic Chemistry*, Berlin, **2010**.
- [3] Z. Guo, P. J. Sadler, *Angew. Chem. Int. Ed.* **1999**, *38*, 1512–1531.
- [4] E. Alessio, Z. Guo, *Eur. J. Inorg. Chem.* **2017**, 1539–1540.
- [5] R. Siegel, *Ca Cáncer J.* **2017**, *67*, 7–30.
- [6] E. Alessio, *Eur. J. Inorg. Chem.* **2017**, 1549–1560.
- [7] P. Zhang, P. J. Sadler, *Eur. J. Inorg. Chem.* **2017**, 1541–1548.
- [8] J. J. Soldevila-Barreda, P. J. Sadler, *Curr. Opin. Chem. Biol.* **2015**, *25*, 172–183.

- [9] C. G. Hartinger, N. Metzler-Nolte, P. J. Dyson, *Organometallics* **2012**, *31*, 5677–5685.
- [10] G. Gasser, I. Ott, N. Metzler-Nolte, *J. Med. Chem.* **2011**, *54*, 3–25.
- [11] P. C. Bruijninx, P. J. Sadler, *Curr. Opin. Chem. Biol.* **2008**, *12*, 197–206.
- [12] M. Arredondo, M. T. Núñez, *Mol. Aspects Med.* **2005**, *26*, 313–327.
- [13] G. Patra, Malay; Gasser, *Nat. Rev. Chem.* **2017**, *1*, 0066–0066.
- [14] B. Albada, N. Metzler-Nolte, *Chem. Rev.* **2016**, 11797–11839.
- [15] B. Albada, N. Metzler-Nolte, *Acc. Chem. Res.* **2017**, *50*, 2510–2518.
- [16] N. Metzler-Nolte, D. R. van Staveren, *Chem. Rev.* **2004**, *104*, 5931–5985.
- [17] N. Metzler-Nolte, M. Salmann, in *Ferrocene* (Ed.: P. Stepnicka), Wiley-VCh, Weinheim, **2008**, pp. 499–639.
- [18] T. Noyhouzer, C. L’Homme, I. Beaulieu, S. Mazurkiewicz, S. Kuss, H. B. Kraatz, S. Canesi, J. Mauzeroll, *Langmuir* **2016**, *32*, 4169–4178.
- [19] C. Lu, J. M. Heldt, M. Guille-Collignon, F. Lemaître, G. Jaouen, A. Vessières, C. Amatore, *ChemMedChem* **2014**, *9*, 1286–1293.
- [20] H. Z. S. Lee, O. Buriez, F. Chau, E. Labbé, R. Ganguly, C. Amatore, G. Jaouen, A. Vessières, W. K. Leong, S. Top, *Eur. J. Inorg. Chem.* **2015**, 4217–4226.
- [21] A. C. Gonçalves, T. S. Morais, M. P. Robalo, F. Marques, F. Avecilla, C. P. Matos, I. Santos, A. I. Tomaz, M. H. Garcia, *J. Inorg. Biochem.* **2013**, *129*, 1–8.
- [22] P. R. Florindo, D. M. Pereira, P. M. Borralho, C. M. P. Rodrigues, M. F. M. Piedade, A. C. Fernandes, *J. Med. Chem.* **2015**, *58*, 4339–4347.
- [23] T. S. Morais, A. Valente, A. I. Tomaz, F. Marques, M. H. Garcia, *Future Med. Chem.* **2016**, *8*, 527–544.
- [24] D. Schlawe, A. Majdalani, J. Velcicky, E. Heßler, T. Wieder, A. Prokop, H. G. Schmalz, *Angew.*

- Chem. Int. Ed.* **2004**, *43*, 1731–1734.
- [25] A. Cingolani, C. Cesari, S. Zacchini, V. Zanotti, M. C. Cassani, R. Mazzoni, *Dalton. Trans.* **2015**, *44*, 19063–19067.
- [26] A. Quintard, J. Rodriguez, *Angew. Chem. Int. Ed.* **2014**, *53*, 4044–4055.
- [27] C. Johnson, M. Albrecht, *Coord. Chem. Rev.* **2017**, *352*, 1–14.
- [28] M. N. Hopkinson, C. Richter, M. Schedler, F. Glorius, *Nature* **2014**, *510*, 485–496.
- [29] S. P. Nolan, Ed. , *N-Heterocyclic Carbenes: Effective Tools for Organometallic Synthesis*, Wiley VCH, **2014**.
- [30] C. Cesari, S. Conti, S. Zacchini, V. Zanotti, M. C. Cassani, R. Mazzoni, *Dalton. Trans.* **2014**, *43*, 17240–17243.
- [31] C. Cesari, R. Mazzoni, H. Müller-Bunz, M. Albrecht, *J. Organomet. Chem.* **2015**, *793*, 256–262.
- [32] C. Cesari, A. Cingolani, C. Parise, S. Zacchini, V. Zanotti, M. C. Cassani, R. Mazzoni, *RSC Adv.* **2015**, *5*, 94707–94718.
- [33] L. Mercks, M. Albrecht, *Chem. Soc. Rev.* **2010**, *39*, 1903–1912.
- [34] S. A. Patil, S. A. Patil, R. Patil, R. S. Keri, S. Budagumpi, G. R. Balakrishna, M. Tacke, *Futur. Med. Chem* **2015**, *7*, 1305–1333.
- [35] W. Liu, R. Gust, *Coord. Chem. Rev.* **2016**, *329*, 191–213.
- [36] T. Zou, C. N. Lok, P. K. Wan, Z. F. Zhang, S. K. Fung, C. M. Che, *Curr. Opin. Chem. Biol.* **2018**, *43*, 30–36.
- [37] T. Fatima, R. A. Haque, M. R. Razali, A. Ahmad, M. Asif, M. B. Khadeer Ahamed, A. M. S. Abdul Majid, *Appl. Organomet. Chem.* **2017**, *31*, e3735.
- [38] K. B. Choo, W. L. Mah, S. M. Lee, W. L. Lee, Y. L. Cheow, *Appl. Organomet. Chem.* **2018**, *32*, e4377.

- [39] M. Pellei, V. Gandin, C. Marzano, M. Marinelli, F. Del Bello, C. Santini, *Appl. Organomet. Chem.* **2018**, *32*, e4185.
- [40] C. R. Shahini, G. Achar, S. Budagumpi, M. Tacke, S. A. Patil, *Appl. Organomet. Chem.* **2017**, *31*, e3819.
- [41] J. Tan, H. Sivaram, H. V. Huynh, *Appl. Organomet. Chem.* **2018**, *32*, e4441.
- [42] B. Blom, G. Tan, S. Enthaler, S. Inoue, J. D. Epping, M. Driess, *J. Am. Chem. Soc.* **2013**, *135*, 18108–18120.
- [43] C. H. Knölker, H.-J. , Heber, J., Mahler, *Synlett* **1992**, *12*, 1002–1004.
- [44] J. Knölker, H.-J., Heber, *Synlett* **1993**, *12*, 924–926.
- [45] J. Knölker, H.-J., Baum, E., Heber, *Tetrahedron Lett.* **1995**, *36*, 7647–7650.
- [46] I. Lohse, E. Wildermuth, S. P. Brothers, *Oncotarget* **2018**, *9*, 35448–35457.
- [47] G. M. Sheldrick, *SADABS-2008/1 - Bruker AXS Area Detector Scaling and Absorption Correction*, Bruker AXS: Madison, Wisconsin, USA, **2008**.
- [48] G. M. Sheldrick, *Acta Cryst.* **2015**, *C71*, 3–8.
- [49] A. L. Spek, *J. Appl. Crystallogr.* **2003**, *36*, 7–13.
- [50] A. L. Spek, *Acta Crystallogr. Sect. D Biol. Crystallogr.* **2009**, *65*, 148–155.
- [51] C. H. R. Martínez, C. Dardonville, *ACS Med. Chem. Lett.* **2013**, *4*, 142–145.
- [52] D. S. Mérel, M. Elie, J.-F. Lohier, S. Gaillard, J.-L. Renaud, *ChemCatChem* **2013**, *5*, 2939–2945.
- [53] H. Allen, O. Kennard, D. G. Watson, L. Brammer, A. G. Orpen, R. Taylor, *J. Chem. Soc., Perkin Trans. 2* **1987**, S1–S19.
- [54] M. Patra, G. Gasser, M. Wenzel, K. Merz, J. E. Bandow, N. Metzler-Nolte, *Organometallics* **2010**, *29*, 4312–4319.
- [55] L. Rigamonti, G. Orteca, M. Asti, V. Basile, C. Imbriano, M. Saladini, E. Ferrari, *New J. Chem.*

2018, *42*, 7680–7690.

- [56] Z. Cruz-Monserrate, C. L. Roland, D. Deng, T. Arumugam, A. Moshnikova, O. A. Andreev, Y. K. Reshetnyak, C. D. Logsdon, *Sci. Rep.* **2014**, *4*, 1–8.
- [57] P. V. Simpson, I. Casari, S. Paternoster, B. W. Skelton, M. Falasca, M. Massi, *Chem. - A Eur. J.* **2017**, *23*, 6518–6521.
- [58] E. Ratzon, Y. Najajreh, R. Salem, H. Khamaisie, M. Ruthardt, J. Mahajna, *BMC Cancer* **2016**, *16*, 1–11.